

APL's Contributions to Stratospheric Ballooning for Space Science

E. Brian Alvarez, Harry A. Eaton, Michael S. Carpenter, Bliss G. Carkhuff, and Pietro N. Bernasconi

ABSTRACT

The Johns Hopkins University Applied Physics Laboratory (APL) has been instrumental in developing stratospheric ballooning for scientific research. Our contributions include systems for unprecedented pointing accuracy and stability that have enabled missions that would otherwise be impossible. In addition, we have engineered systems for avionics, power, software, command and control, ground support, integration, and testing. APL staff members have worked in the field to integrate, troubleshoot, and operate the balloon systems. These accomplishments have supported innovative space science missions in heliophysics, astrophysics, and planetary science.

INTRODUCTION

For the past 26 years, what is now called the Electrical and Mechanical Engineering Group in APL's Research and Exploratory Development Department (REDD) has partnered with the Lab's Space Exploration Sector to make major contributions to stratospheric balloon science systems. Starting in the mid-1990s with the Flare Genesis Experiment (FGE),^{1,2} and with three current balloon missions under development (Galactic/Extragalactic ULDB Spectroscopic Terahertz Observatory, or GUSTO; Sunrise III; and Astrophysics Stratospheric Telescope for High Spectral Resolution Observations at Submillimeter-wavelengths, or ASTHROS), we have been involved in over a dozen missions focused on all three pillars of space science—astrophysics, heliophysics, and planetary science. The ability to execute scientific inquiry from an inexpensive balloon platform enables missions that lack funding for a rocket-launched space-based scientific platform.

This article describes APL's evolution in stratospheric ballooning missions and how our solutions to major

technical challenges have enabled significant scientific study. APL's efforts have been critical to developing and growing mission parameters and to delivering the technical achievements required to enable and sustain them. Our major contributions include telescope pointing, command and control, power, and ground support systems. In addition, we have supported electrical and mechanical hardware manufacturing, software design, and testing for flight and ground systems, field support, and mission operations. This article focuses on our key contributions to advancing critical subsystems, as well as our field and mission operations.

BACKGROUND

Scientific balloons are large, uncrewed, helium-filled balloons. A fully expanded scientific balloon has a volume of ~40 million ft³ (Figure 1)—a space large enough to contain more than 195 blimps.³ These balloons reach altitudes of ~120,000 ft,³ between three

and four times the flight altitudes of typical commercial passenger aircraft. This altitude puts floating scientific balloons firmly in the stratosphere of Earth's atmosphere; hence the more specific moniker for scientific ballooning—stratospheric ballooning. While floating in the stratosphere, the balloon is protected from the harshest environmental conditions of outer space, but it is elevated above most of the detrimental atmospheric effects that limit (and sometimes prevent) scientific observations from ground-based systems. This “Goldilocks Zone” provides unique opportunities for scientific instruments that would be ineffective from the ground and unfeasible for use in satellites and spacecraft. Not to mention, hitching a ride on a balloon up to the stratosphere is significantly more affordable than catching a ride on a rocket into outer space.

These stratospheric balloons, while impressive in their own right, would not be nearly as useful for research if not for their ability to carry scientific instrumentation. Science payloads, up to 8,000 lb, are suspended from the bottom of the balloon.¹ Being able to support such heavy loads means that a variety of telescopes and other

scientific instrumentation can fly (suspended) from the balloon.

The telescopes and science instruments typically require a support structure around them, called a gondola (Figure 2). The gondola provides a suspension point to attach to the balloon, as well as housing systems to control/point, power, thermally regulate, and communicate with the science instrumentation. This is the area in which APL has carved a niche in the scientific ballooning community. APL-designed gondola pointing control systems have demonstrated some of the most accurate and stable pointing ever achieved from a balloon-borne platform.⁴

The gondola on APL's most recent ballooning mission, STO-2, had pointing accuracy within 10 arcsec, with extended periods of observation with 0.51 arcsec root mean square (RMS) jitter. This is the equivalent of maintaining telescope aim on the face of a dime from 2.3 mi (3.67 km) away, all while being suspended from a floating (that is, moving) balloon. This pointing accuracy and stability is why other research institutions seek to partner with APL to achieve their balloon-borne science goals.

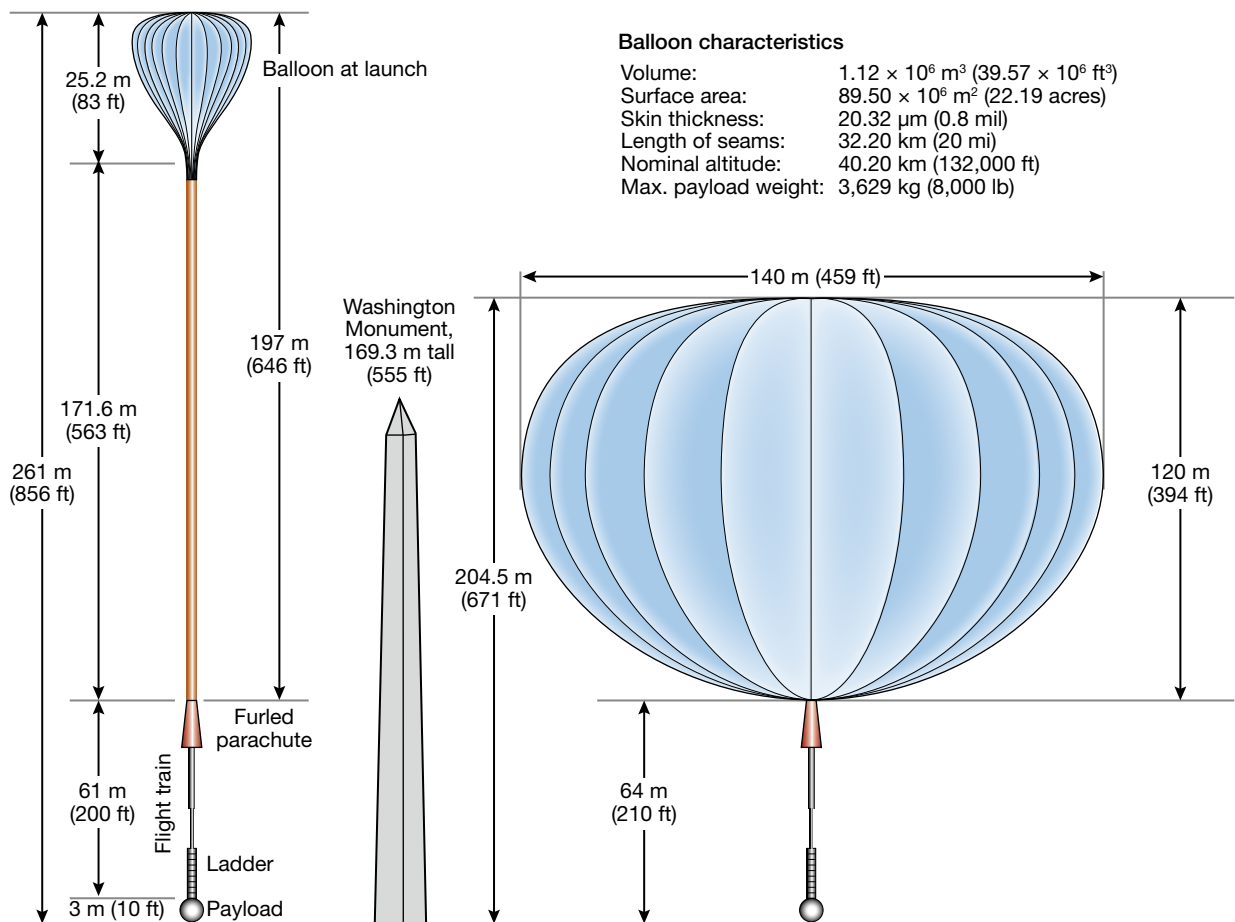


Figure 1. Scientific balloon dimensions. A stratospheric balloon with a payload attached towers more than 100 ft (~30 m) taller than the Washington Monument. It can carry scientific payloads up to 8,000 lb (3,629 kg). (Graphic adapted from a NASA Balloon Program Office graphic.)



Figure 2. Anatomy of a balloon gondola. The gondola supports telescopes and other scientific equipment. This gondola from the second Stratospheric Terahertz Observatory II (STO-2) mission is 22 ft (6.7 m) tall and weighs 5,200 lb (2,358 kg). It houses solar arrays, telescopes, and other equipment necessary to power and control the scientific instrumentation.

HISTORICAL OVERVIEW

Our involvement in stratospheric ballooning started in the early 1990s, in collaboration with an APL solar scientist, on a NASA grant for the FGE (Figure 3). The grant included a basic mechanical design with mechanisms from the Harvard & Smithsonian Center for Astrophysics, including a gondola and a main telescope with a primary mirror 0.8 m in diameter. The system was an altitude (elevation)–azimuth design, where the telescope tilted within the gondola in altitude and the entire gondola was oriented in azimuth to aim at the desired location. Our team adapted existing technology to aim at various solar regions active with sunspots. A 1996 Antarctica flight demonstrated the ability to acquire and track active regions on the Sun.

The system flew again in 2000 with a number of our team's design improvements, including a fine-motion compensation system using a fast tip-tilt mirror driven by voice-coil actuators to remove residual pointing jitter from the main telescope image. This increased overall image resolution and signal-to-noise ratio (SNR) by limiting the motion smearing during long exposure times. Also, we modified the azimuthal actuator (known as the momentum transfer unit, or MTU for short) based on Newton's third law to directly shed excess angular momentum into the balloon cable instead of trying to produce equal and opposite torques in two different motors. This design change greatly reduced the amplitude of the periodic azimuth disturbances that occurred

whenever momentum transferred from the azimuth reaction wheel (used to steer the gondola in azimuth) into the balloon cable. The successful 2000 flight informed several scientific papers⁵ and led to more balloon projects in collaboration with various institutions.

The FGE success led to another solar science grant, for the Solar Bolometric Imager (SBI),² flown in 2003 and 2007 (with a failed flight in 2006). This mission was a collaboration with Heliophysics, Inc. Our team provided the gondola and solar pointing system and also developed the instrument interface, optical filter wheel, and data acquisition and storage system. SBI measured the total irradiance from the Sun across the full spectrum

while characterizing the variation from sunspots, faculae, and the solar granulation network. Results included ultra-wideband imagery of the total energy of the solar disk, as well as infrared (IR) to ultraviolet (UV) calibration of these data.⁶

APL's reputation for excellent pointing and stability led to a collaboration with the University of Arizona for STO,⁷ an astrophysics grant project to survey cold and warm gas clouds in the galaxy. This project required many new developments to point at arbitrary locations in the sky with no visible targets. We developed a star camera that worked at balloon altitudes. Commercially available star cameras only work outside the atmosphere or at night, when contrast between star and sky is high. At balloon altitudes over Antarctica, during the day the sky is still quite bright, making stars difficult to see. In addition to the star camera needed for determining absolute reference positions, we developed a measurement system using fiber optic gyroscopes to track changes in the telescope position. Our team also developed the software necessary to combine these elements into a telescope pointing system that could scan across the sky and track calibration targets such as planets and nebulae. Additional modifications to the MTU allowed for continuous shedding of momentum, further reducing pointing jitter. STO flew successfully in Antarctica in 2012; the pointing control system worked well, but instrument problems limited the scientific value of the data obtained.

					
FGE	SBI	BRRISON and BOPPS	STO	GUSTO	Sunrise III
Solar physics	Solar physics	Planetary physics	Astrophysics	Astrophysics	Solar physics
80-cm-diameter solar telescope with solar vector magnetograph	20-cm-diameter solar telescope with solar bolometric imager	80-cm-diameter optical telescope with visible and IR multispectral cameras	80-cm-diameter far-IR telescope with cryogenic IR (THz) spectrometer	93-cm-diameter far-IR telescope with cryogenic IR (THz) spectrometer	100-cm-diameter solar telescope with solar vector magnetograph and 2 polarimetric spectrographs
Stratospheric flights: 1994: 1 day (test) 1996: 19 days 2000: 17 days	Stratospheric flights: 2003: 1 day 2006: 1 day 2007: 1 day	Stratospheric flights: 2013: 1 day 2014: 1 day	Stratospheric flights: 2009: 1 day (test) 2012: 14 days (STO-1) 2016: 22 days (STO-2)	Stratospheric flights: 2022: up to 75 days	Stratospheric flights: 2022: up to 6 days

Figure 3. History of scientific stratospheric ballooning at APL. Beginning in 1994 and continuing through the present day, APL has contributed to several scientific ballooning missions with solar physics, planetary physics, and astrophysics goals. These missions had flights ranging from 1 day up to 75 days.

STO's excellent pointing led to another ballooning opportunity, this time in planetary science with an ephemeral target. The Balloon Rapid Response for ISON (BRRISON) mission was conceived and executed incredibly quickly to study the comet ISON, a recently discovered comet predicted to pass near Earth only once and only about a year after its discovery. BRRISON reused many components from STO but required some new systems and improvements. For example, our team developed a roll-stabilization system to further reduce pointing jitter so that long exposures could be used to see ISON's dim IR energy, which would have a very small angular size. BRRISON launched in Fort Sumner, New Mexico, in 2013. Although BRRISON demonstrated low jitter (<1 arcsec peak) while observing a star during commissioning, an anomaly ended the mission before it could attempt to observe the comet.

On the heels of BRRISON, and spurred by the arrival of two Oort cloud comets in 2013 and 2014, our APL team created and flew the Balloon Observation Platform for Planetary Science (BOPPS). This gondola, which weighed 5,200 lb, stood 22 ft tall, and measured 8 ft wide at launch, used advances in tracking and stabilization to collect data on comets Siding Spring and PANSTARRS, the asteroid Ceres, and different types of stars from a balloon-mounted telescope operating at up to 125,000 ft above Earth. Before BOPPS and BRRISON, planetary science balloon missions had not been attempted in 40 years, largely due to the difficulty in achieving the

required pointing precision. BOPPS successfully flew in 2014 from NASA's Columbia Scientific Balloon Facility (CSBF) in Fort Sumner, New Mexico. The mission proved the viability of making difficult scientific measurements from a balloon platform affordably and with a rapid response time.

These demonstrated capabilities led to the grant for STO-2, which flew in Antarctica in 2016 with the latest pointing system and instrument improvements. For 20 of the 22 days of flight, STO-2 successfully mapped the Eta Carinae nebula in the one-time ionized carbon emission line at $158 \mu\text{m}$.⁸ Preliminary scientific results would go on to support the winning proposal for NASA's GUSTO mission, which is scheduled for a 55- to 75-day flight in 2023. GUSTO is the most expensive balloon mission yet undertaken. Our team is developing a next-generation star camera and a distributed peak-power-tracking power management system for GUSTO's solar arrays. We are also improving the system simulator, a software model initially developed during BRRISON that simulates the dynamics of the gondola structure and mechanisms, the power system (solar and batteries), and the flight path. The simulator allows the vast majority of the actual flight code (including real-time control loops), command and control, and many other components to be tested with full mission parameters. We are adding a star camera simulation, which generates simulated sky images that pass through the flight star camera software as if they came directly from the imager, and also

a thermal model that shows how various component temperatures change during the mission, including day/night cycles. These new features are just the highlights of several improvements developed by APL.

Our team is also developing the pointing control, command and control, power, and ground support subsystems for Sunrise III, another NASA grant balloon project, in collaboration with the Max Planck Institute for Solar System Research in Germany. Sunrise III is a heliophysics mission with a 1-m-diameter solar telescope featuring two spectropolarimeters (one UV and one visible-infrared) and an imaging magnetograph. Previous Sunrise flights have been limited by inadequate pointing accuracy and stability, which led to Max Planck seeking out APL for collaboration on this latest iteration. Sunrise III attempted a launch in Sweden in June 2022, but there was an anomaly with the launch vehicle. A new mission is being formulated for launch in June 2024.

APL has also been awarded a grant for ASTHROS, which started in the fall of 2021. ASTHROS is a 2-m terahertz telescope for astrophysics science being developed by NASA's Jet Propulsion Laboratory (JPL). JPL will provide the telescope and science instruments, and our team will be responsible for everything else (gondola, pointing control, power, command and control, thermal, etc.).

CRITICAL SUBSYSTEM EVOLUTION

With each successive ballooning mission, new capabilities have been added and existing ones have been improved. This evolution is particularly noteworthy in the pointing control subsystem, attitude estimation capabilities, and power subsystem. These subsystems' current statuses are briefly discussed below.

Pointing Control System

All of APL's major stratospheric balloon projects have had telescope-based science instruments. The gondola supporting the telescope hangs from the flight train beneath the balloon (Figure 1). Because the gondola is hanging beneath the balloon, it is generally oriented upright relative to the local Earth surface below. This vertical gondola orientation naturally suggests an elevation-azimuth (often called altitude-azimuth or alt-az; Figure 4) telescope pointing actuation used by APL and other groups flying balloon telescopes. Compared with spacecraft, balloons get one axis of orientation almost for "free," but they are subject to much larger disturbances than spacecraft.

The balloon travels freely with the wind and can travel hundreds or thousands of miles during a mission (refer to Figure 17). When the balloon is first launched, it takes several hours to rise to the "float" altitude and then it "bounces" around in altitude for another hour

or so before it stabilizes to a slowly varying altitude profile dictated by thermal changes as the Sun changes elevation in the sky. The air pressure at float altitude is typically around 5 mbar. This low pressure means that the force of wind on the gondola is greatly diminished compared with at ground level. In addition, since the balloon travels with the wind, the average wind force across the whole system does not disturb it much. Wind disturbances are mainly due to the differences between the winds blowing on the payload compared with those blowing on the balloon.

The flight train (refer to Figure 1) is quite long—on the order of 60 m or more—but total length and mass vary across missions. An in-line parachute at the top of the flight train attaches to the balloon through a release mechanism, and a fairly long ladder-like steel cable assembly attaches to the bottom of the parachute cords through another release mechanism. At the bottom of the ladder, a truck-plate and a few short steel cables connect to the gondola. This long flight train with the gondola hanging at the bottom naturally forms a compound pendulum system. This complicated system has many different modes of oscillation,⁹ most of which have little damping. In most cases, the pendulum behavior exacerbates telescope aiming errors caused by the wind. The overall pendulum angular deviations during a typical flight are on the order of 0.1°.

In an alt-az system (Figure 4), any deviation of the "telescope mount" from true vertical introduces errors in the telescope aim, so balloon telescopes need to continuously correct these errors. Errors in elevation are easier to manage than those in azimuth because usually the

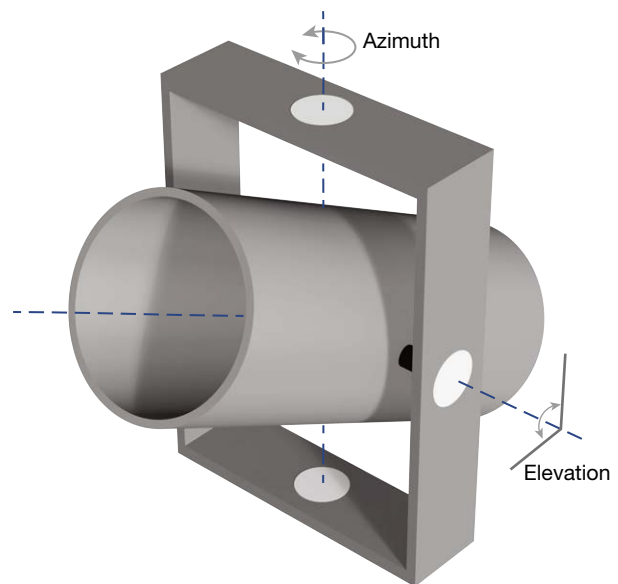


Figure 4. Typical alt-az (elevation-azimuth) mount for a balloon telescope. An alt-az mount allows for rotation on the vertical axis to vary the azimuth of the pointing direction, while rotation on the horizontal axis varies the altitude angle, or angle of elevation.

telescope's target, and thus desired position, is stationary (or nearly stationary) in inertial space. The telescope's own inertia resists the disturbance, and residual motion of the gondola about the stabilized telescope's elevation axis tends to dampen any pendulum motion along that direction.

The azimuth axis is more complicated. Unless there is a gimbal between the gondola and the telescope that can compensate for side-to-side pendulum motions, the entire gondola has to be rotated to compensate for those motions and prevent pointing errors. Some high-resolution balloon telescope gondolas use a two-axis gimbal system to achieve high-accuracy pointing.^{10,11} These systems roughly stabilize the overall gondola pointing and then drive the telescope/payload with the gimbal to correct the residual error. The main drawback of a gimbal system is that it is very difficult to accommodate large-diameter telescopes. The challenge is that the gimbal must be larger than the telescope but also fit inside the gondola or the entire telescope must be in front of the gimbal with corresponding counterbalance mass behind the gimbal. Since APL's first balloon project used a large telescope where gimbals were impractical, APL's pointing system is designed to stabilize the entire gondola.

Our pointing control system (Figure 5) uses a direct-drive torque motor on the elevation axis to stabilize the telescope elevation. This requires that the telescope/instrument system be well balanced so that its center of gravity is on the elevation's rotation axis. For payloads that have cryogenics that boil off over the life of the mission (like STO-2 and GUSTO), we control the position of a sliding mass to adjust the telescope balance. The control for this measures the average control torque minus any torque that is intended to accelerate the telescope to a new position and then uses a proportional-integral control equation to adjust the slider position to zero this average torque.

The azimuthal actuator is called the momentum transfer unit, or MTU (Figure 6), because it must shed any momentum that the wind imparts to the gondola. The MTU is at the top of the gondola and provides the attachment point to the flight train. It uses a large reaction wheel driven by a motor on the gondola to provide steering torques that rotate the entire gondola in azimuth. As the wheel gains speed, its momentum transfers to the flight train and eventually to the balloon itself through a shorted motor connected between the reaction wheel and the suspension point. The MTU

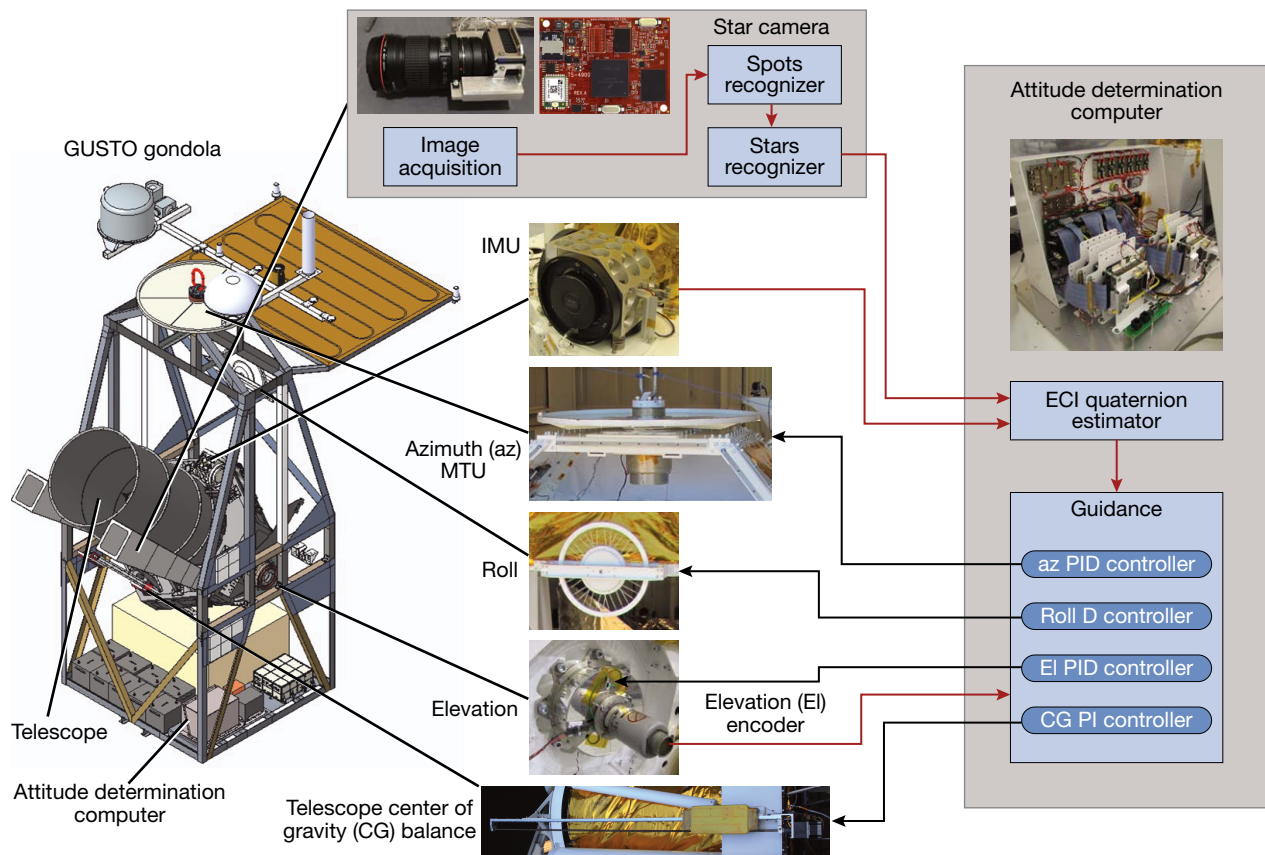


Figure 5. Elements of the APL-developed balloon pointing control and attitude determination system for astrophysics missions. This system stabilizes the telescope elevation and ensures that the telescope remains pointed at its intended target. IMU, inertial measurement unit; ECI, Earth-centered inertial; PID, proportional, integral, and derivative action.

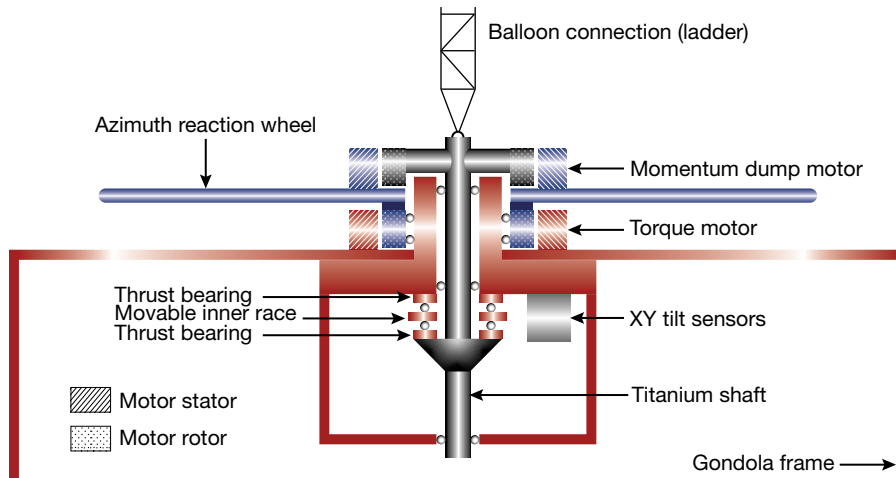


Figure 6. MTU schematic. Located at the top of the gondola, the MTU sheds any momentum imparted on the gondola by wind. In addition to the gondola, it accommodates rotation on the azimuth axis from the reaction wheel (blue) and the flight train.

has to accommodate three rotating elements about the azimuth axis: the gondola, the reaction wheel, and the flight train. At any given moment, each rotates with its own direction and speed independent of the other two. The gondola and the flight train always rotate slowly, while the reaction wheel can spin much faster. This behavior allows the shorted motor to automatically adapt the torque and shed excess wheel momentum into the flight train.

The gondola system's large momentum of inertia about the azimuth axis limits the speed that it can rotate to correct for side-to-side (gondola roll) pendulum motions. The pendulum's higher-frequency modes (e.g., the mode where the gondola pivots about its center of gravity), if left undamped, can often be too fast to be corrected by rotating the gondola in azimuth. Accelerating the gondola azimuth may also add energy to the pendulum motion² because of imprecise gondola balance and other imperfections in the system. APL's early missions did not have any means to deal with these motions, which were the limiting factor in pointing accuracy in the FGE and SBI missions. APL has solved this problem by implementing a dynamic system that dampens oscillation about the gondola roll axis. Other balloon projects have tried passive pendulum damping techniques such as mounting a pendulum with large mass immersed in oil to the gondola.⁴ Our system (Figure 7) uses a motor-driven reaction wheel mounted along the gondola's roll axis (the roll wheel). It is driven by a control system that produces torque proportional to the roll angular velocity (measured by fiber optic gyroscopes) but in the opposite direction, which is a pure damping term in the equations of angular motion. The lowest-frequency modes of the flight train pendulum can have periods longer than 20 s. Because of mass limitation on the roll wheel, these

low-frequency modes can easily saturate its speed and render it ineffective for correcting the higher-frequency modes. However, the low-frequency modes are slow enough that azimuth rotation of the gondola can correct the pointing errors from them. Our control system applies a notch filter (along with phase correction above the notch) to ignore the lowest-frequency pendulum oscillations. We also subtract any constant gondola roll rate due to Earth rotation before computing the control torque. The limited roll wheel moment of inertia also means that it takes several minutes to dampen oscillations down to

the arcsecond level, making it important to minimize exciting them in the first place.

Many balloon missions APL has supported have required aiming the telescope at various places across the sky, while others have been solar missions that spend all of their time looking at the Sun or a small portion of it. In the first case, the telescope must move through large angular distances to get to different targets of interest,

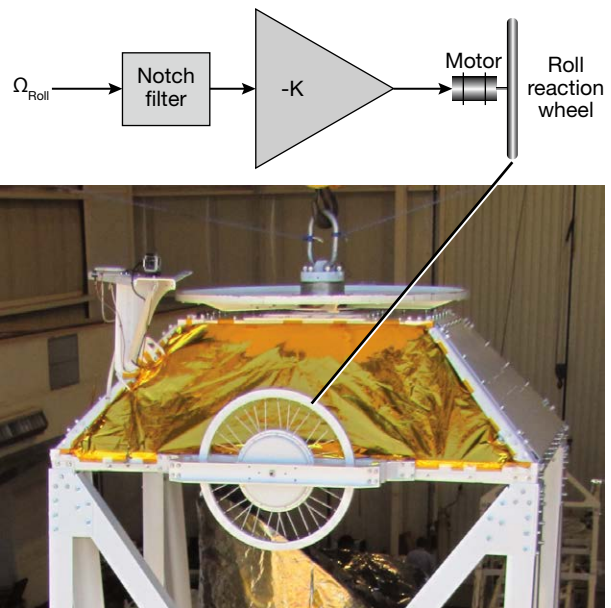


Figure 7. Roll-stabilization system schematic. This system helped overcome the main limiting factor to pointing accuracy in early balloon missions—that is, pendulum motion of the gondola. Rather than being a passive system, this system produces torque proportional to the roll angular velocity, but in the opposite direction.

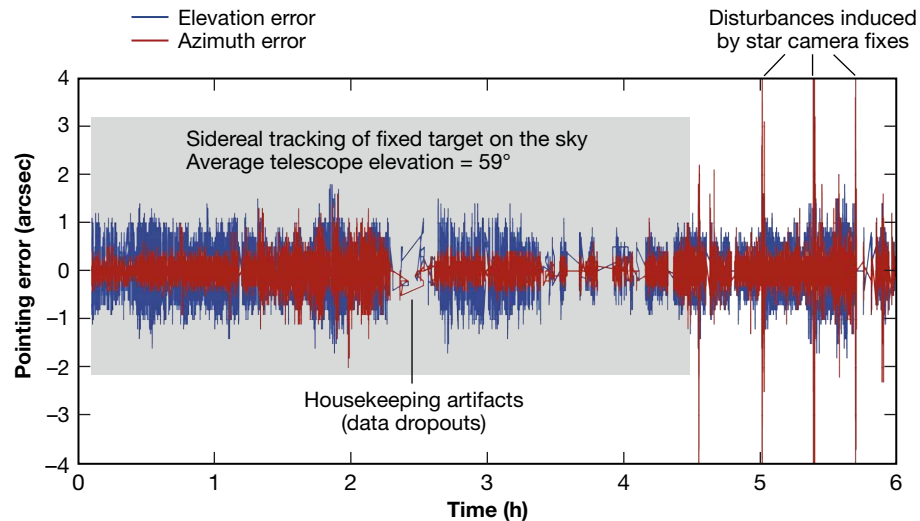


Figure 8. Telescope pointing errors in azimuth and elevation on a 6-h period during the STO-2 flight in 2016. During this time, the STO-2 telescope was pointed at a fixed target on the celestial sphere. The RMS pointing error over this period was 0.44 arcsec in elevation and 0.27 arcsec in azimuth.

whereas in the latter case, the telescope has to make large movements to acquire the Sun initially or reacquire it if it is lost. As described earlier, angular accelerations can contribute to undesirable pendulum oscillations. Our control systems implement acceleration- and jerk-limited control during large maneuvers to proactively minimize exciting the pendulum modes; without this, damping the pendulum oscillation would take many cycles. We have balanced the acceleration limits that increase the time to get to a target with the damping time necessary to stabilize once there before starting observations. With these pointing control system features, we have achieved very low jitter errors in the telescope pointing. Figure 8 shows the performance during typical STO-2 observations.

Attitude Estimation

No matter the target, a telescope requires accurate pointing, which begins with knowing where the telescope is pointed in the first place. This is the task of attitude estimation.

Sun-Guided System

For solar missions (FGE, SBI, Sunrise III) we use a Sun-guider system (Figure 9) to precisely point the telescope at the Sun. The first step is coarsely acquiring the Sun. To do this, the gondola rotates in a circle, and a pair of wide-angle ($\sim 15^\circ$) sensors wait for a signal that indicates the Sun is in their field of view. From these sensors' feedback, the telescope can be centered close enough to the Sun that the Sun-guider telescope can take over. The Sun-guider telescope produces a full-disc solar

image (~ 1 cm in diameter) that shines onto a quad-cell photo diode detector. The quad-cell detector is able to measure arcsecond-level offsets of the solar image.

The control equations that drive the azimuth and elevation control systems regulate the solar disc image in the center of the quad-cell detector at all times. The detector is mounted on a two-axis linear motion stage (XY stage) that allows the telescope to be aimed at different parts of the Sun. Once the guide telescope acquires the Sun, the two-axis stage is offset to precisely locate the upper, lower, left, and right limbs of the solar disc in the main telescope image. When all the solar

limbs have been accurately found, the control system tracks and updates the telescope attitude as time elapses, the gondola's position over Earth changes, and the XY stage either moves to a new region of the Sun or adjusts to remain on a particular solar feature.

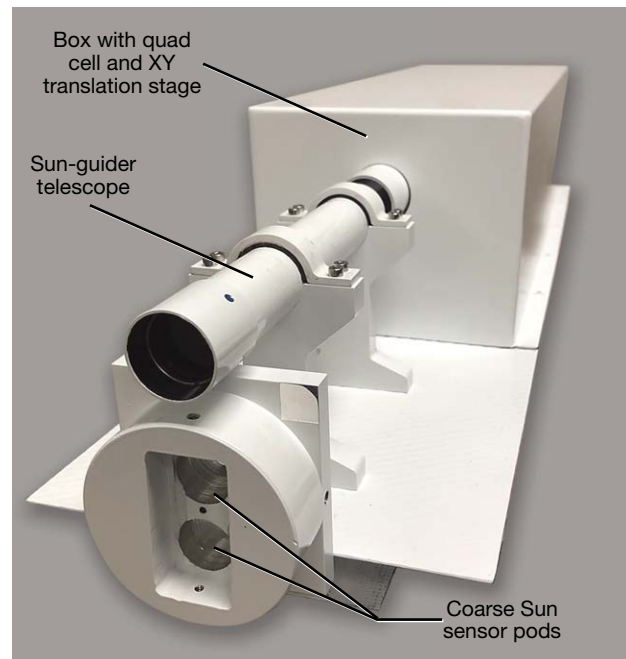


Figure 9. Sunrise III Sun-guider system. Once it is centered close enough to the Sun, the telescope produces a full-disc solar image that shines onto a quad-cell photo diode detector. The quad-cell detector is then able to measure arcsecond-level offsets of the solar image.

Star Camera—Inertial Measurement Unit System

Astrophysics and planetary mission observation targets are much more subtle than the Sun, requiring a far more complicated means of attitude estimation that is applicable anywhere on the celestial sphere. For such missions, the primary feedback source for telescope movement is a trio of orthogonally oriented high-precision fiber optic gyroscopes mounted directly onto the telescope, referred to as an inertial measurement unit (IMU) (Figure 5). The gyroscopes provide subarcsecond/second-level precision of telescope velocity. However, this movement needs to be translated relative to the telescope onto the celestial sphere—where observational targets are represented in Earth-centered inertial (ECI) coordinates. This is the role of the attitude quaternion.

Quaternion math is a powerful tool for describing the rotational relationship between two different frames of reference. It provides a computationally succinct way to rotate a 3-D vector from one frame of reference to another while avoiding common pitfalls, such as gimbal lock and matrix regularization, from accumulated computational error that can occur with other rotation methods. The attitude quaternion describes the rotation necessary to transform vectors in telescope body coordinates into vectors in ECI coordinates. This allows for the path between two points on the celestial sphere to be translated into movements relative to the telescope, which can then be broken down into the azimuthal and elevation components that the control system actuates to drive the telescope.

The attitude quaternion is continuously updated based on the SO(3) integration measurements of the fiber optic gyroscopes [SO(3) is a special orthogonal group representing 3-D rotations]. Although the gyroscopes provide subarcsecond/second-level precision, they are not perfect. Like any system that relies on integrating measurements to determine position, measurement errors accumulate over time. The quaternion's coarse validity is constantly checked by requiring that it provide a nearly vertical gondola for the current GPS position and that the telescope elevation angle is close to that measured by the shaft angle encoder between the gondola and telescope. If the quaternion is not valid, a completely different control algorithm using the shaft encoder and a magnetometer-measured azimuth is used to control the telescope. Ideally, errors in the quaternion are small enough that this never occurs. The errors introduced into the quaternion from gyroscope measurements can be reset by comparing the quaternion to an absolute reference of position provided by images taken by an APL-developed star camera. As long as the images contain a sufficient number of stars, they precisely indicate where the telescope is currently pointing on the celestial sphere. Under typical operating conditions for our gondola, star camera images are required only about every 10 min to maintain a high-accuracy quaternion.

Star Camera

Many commercial star cameras are available, but they are intended for space applications with no sky brightness. In the case of balloon missions, the balloon supports the gondola by displacing air with helium, which means there must still be a large air mass at the altitude where the telescope flies. This air mass scatters light from the Sun, creating considerable (compared with starlight) sky brightness during the daytime—and balloon missions operate mostly during daytime because they are solar powered. Since commercial star cameras cannot operate in these bright-sky conditions, APL developed its own.

Sky brightness contributes to poor SNR for starlight. Care must be taken to remove the effects of nonuniformity in the detector element gains and gradients in the observed sky brightness due to vignetting from the camera optics. Both effects are nearly constant for a given camera/lens system, or at least slowly varying, so the system typically only needs to be calibrated once at the beginning of the mission to remove these adverse effects from sky images. Then the star camera's daytime noise level should be dominated by the photon noise in the sky brightness.

APL's star camera (Figure 10) uses multiple strategies to maximize the starlight SNR. First, its deep red filter blocks much of the sky brightness because sunlight is much more strongly scattered at short wavelengths (the sky is blue!). This filter blocks some of the star's light too, but most stars tend to emit mostly in the red part of the spectrum, so a red filter generally improves the SNR.

We chose our camera and optics to ensure a small solid angle of view on the sky for each pixel, which reduces the noise from the sky brightness in each pixel. This shrinks the camera's entire field of view. Other daytime star cameras have very small fields of view for this reason. Ideally, there is no trade-off because as the field of view decreases, it is possible to see dimmer stars. If stars were uniformly distributed over space, the number that could be seen in the camera would not change. But stars are not uniformly distributed, so shrinking the field of view too far risks not having enough visible stars in the image. The accuracy and reliability of the attitude determination increases as more stars are used in the calculation, so seeing several stars in a single image is desirable. Using a detector with many pixels allows a larger view of the sky while the view of each pixel (and thus the sky brightness it sees) is small—but this also has costs. The optics that can achieve a small spot size and wide field of view have more lens distortion and therefore require more accurate calibration, and the many pixels increase readout and image processing times.

Our camera's detector and optics are also constrained so that the lens's spot size (the smallest spot of light produced from a point source at infinity) is about four times the size of a single pixel on the detector. This ensures

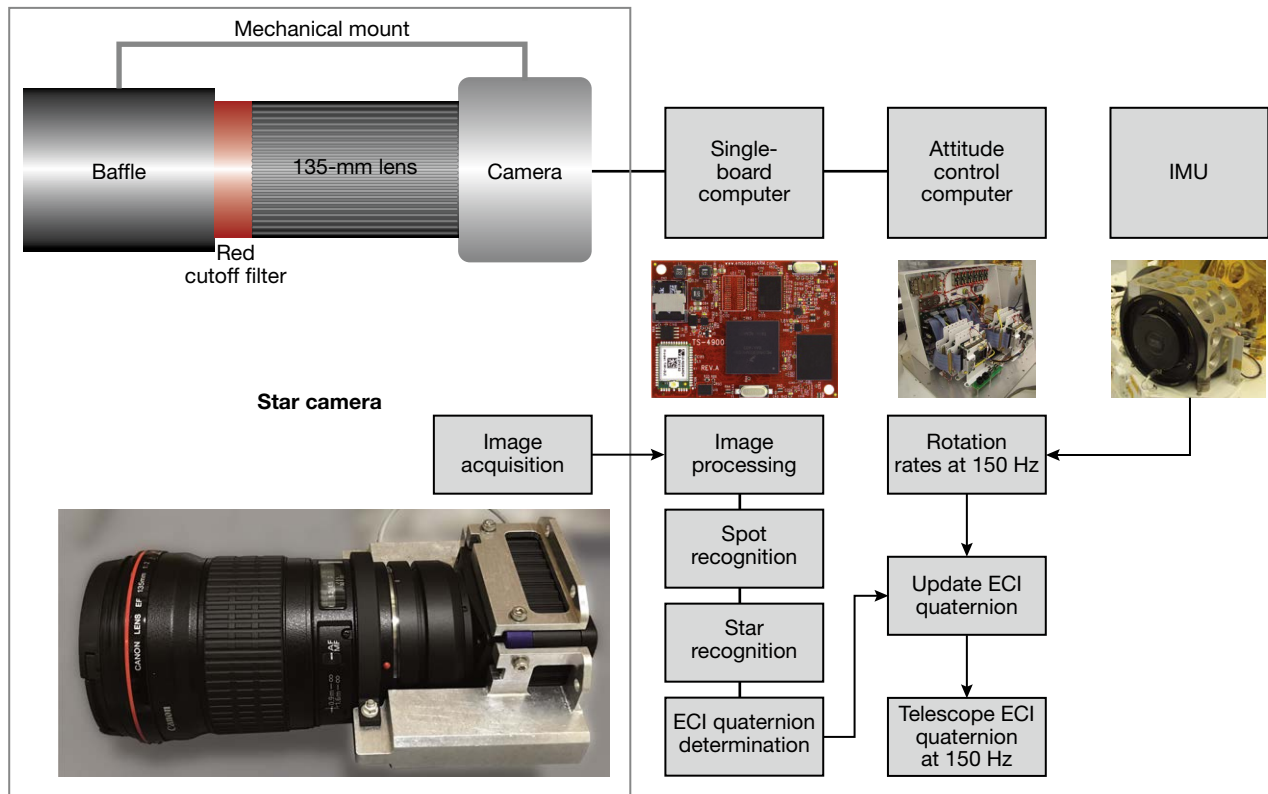


Figure 10. APL-developed daytime star camera system for balloon missions. Unlike commercially available star cameras, this star camera allows for viewing stars even with significant amounts of sky brightness thanks to its red cutoff filter.

that a star's light is spread across only a few pixels but never falls entirely in a single pixel. If all of a star's light went into a single pixel, it would have the highest SNR but it would not be possible to locate its position to sub-pixel accuracy. If instead the starlight is spread across at least four pixels, accuracy close to 0.1 pixel diameter is possible.¹² If the spot size is too small for the detector's pixel size, it is possible to slightly defocus the image to spread the starlight across multiple pixels.

Finally, we opt for a relatively large integration time. The energy gathered from a star increases linearly with integration time, but the photon noise from sky brightness only increases with the square root of the integration time. The maximum integration time is limited by the combined star and sky brightness and the dynamic range of the camera as well as the telescope motion that can smear the star's light across more pixels. The sky brightness varies depending on the angle between the Sun and where the camera is looking, so the exposure time is variable. We usually set it so that the sky brightness takes up about 50% of the detector's dynamic range. This results in integration times up to 600 ms, which means that to prevent smearing during the exposure, the telescope goes into a stationary sidereal tracking mode when it takes a star camera image. This works well for our system because our IMU is highly stable, so it is not necessary for the star camera to have a fast update rate.

Our newest star camera design for GUSTO (Figure 10) uses a near-IR response enhanced 12-megapixel detector with $4.5 \mu\text{m}$ by $4.5 \mu\text{m}$ pixels. We use a commercial Canon EF 135-mm $f/2$ lens, which has a spot size of approximately $18 \mu\text{m}$. This results in each star's light spreading across at least 16 pixels. Although this is not optimal, it is a reasonable trade-off. The full camera field of view on the sky is an 8° by 6° rectangle. A long baffle tube (typically 4–5 ft long) in front of the lens prevents scattered light from the telescope and gondola structure as well as off-axis sky brightness from entering the lens.

Star Recognition

The star camera takes images of the sky, processes them, identifies and finds the SNR and centroid of spots of light that may be stars, and then uses a star recognition algorithm. This algorithm identifies which spots correspond to which stars in a star catalog, then computes a quaternion that produces a weighted (by SNR) best fit for the star camera's orientation in inertial space. We use three strategies to identify the stars, all of which rely on a highly efficient algorithm for querying the star catalog database.¹³ Queries specify a vector touching the unit sphere (representing a direction looking at the sky) and an angular radius about that vector. The query returns a list of stars within the vector's radius. A callback function can add nearly any additional criterion

to the search, such as star magnitude, angular distance from another vector, and so forth. The callback can also terminate the search early if desired.

The first strategy for recognizing stars assumes that the existing attitude quaternion is close to correct, so it transforms the camera body vector of each prospective spot of light into inertial space with the existing attitude, then searches a small (~ 2 arcmin) radius around that vector for the brightest star. As long as several spots of light in the image have corresponding stars and the quaternion estimated from using those stars provides a valid quaternion, the attitude estimate is successful.

If the first strategy fails, we use a different algorithm that is similar to the first, but for each spot of light, it finds a list of stars within a larger radius ($\sim 1^\circ$). For each star in the list, it computes the vector difference between the star's position and the light spot's position. Then a *k*-means clustering algorithm¹⁴ finds the set of different vectors having about the same magnitude and direction. The stars corresponding to this set of vectors are then selected as the true star identities, and the quaternion estimate is computed and validated. This algorithm still assumes that the initial attitude is basically correct but may have a larger offset than the first algorithm can accommodate.

If the second algorithm fails, we are considered to be "lost in space." In that case, we still have the benefit of knowing that we are hanging vertically from a balloon cable, unlike spacecraft, and know reasonably well what the telescope elevation angle is. This knowledge, combined with our GPS position, allows us to create a table of stars that lie within the elevation band that we might see from any azimuth. We measure the angular distance between pairs of light spots in the image and compare those with precomputed pairwise distance tables of catalog stars brighter than magnitude 7.5 that are also in the table of stars in the elevation band. For each pair with similar angular separation between the catalog and the image, we calculate two test quaternions (one for each spot-to-star mapping) using the TRIAD algorithm¹⁵ and then see if either produces a valid quaternion. If a valid quaternion is found, it is used in the first algorithm to recognize the other stars.

Stratospheric Balloon Power System

The four main elements of any balloon power system are batteries, solar panels, maximum power point trackers (MPPTs), and a power distribution unit (PDU). Figure 11 depicts the GUSTO power system.

Batteries

Regardless of a balloon mission's flight duration, batteries are the principal power source. On 1-day missions, such as qualifying flights that last less than 12 h, the CSBF provides the batteries. Each battery consists of 10 lithium-sulfur dioxide cells. Each cell provides 30 A h

of current at ~ 3 V, resulting in a battery bus voltage of 28 V. We have connected 18 of these batteries to provide a capacity of 540 A h for the qualifying flights and 26 to provide a capacity of 780 A h for slightly longer 1-day science missions lasting up to 24 h.

Long-duration missions lasting many days or several weeks require rechargeable batteries. On the SBI and STO-1 and -2 flights, we used 12-V lead-acid absorbed glass mat automotive batteries. Two were used in series for a 24-V bus on the SBI flight to provide 68 A h capacity, and four of these batteries, two-series strings connected in parallel, were used for the STO flights to provide 136 A h of capacity. The GUSTO mission is expected to last around 75 days. Due to the circulation of the stratospheric winds, the first 40–45 days will be spent circling Antarctica with constant sunlight. This allows the batteries to continuously recharge via solar panels. However, the winds will eventually carry the balloon northward into the mid-latitudes, and the gondola will begin to experience periods of darkness as the Sun rises and sets during the orbit. The battery system must be able to provide power during the expected 10 h of darkness. This requires a battery system with much higher capacity. Our estimated nighttime capacity requirement is around 550 A h, so we will use a SAFT 25.5-V, 80-A h lithium iron phosphate battery.

GUSTO will include nine of these batteries connected in parallel for a total capacity of 720 A h, weighing ~ 410 lb. The equivalent in absorbed glass mat batteries would require 22 batteries (11 strings of 2 batteries in series) weighing $\sim 1,342$ lb. Additionally, each SAFT battery has a built-in battery management system, which protects against overvoltage charging, undervoltage discharging, overcurrent discharging, and over-temperature shutdown. Information regarding the health and status of each battery is provided over a CAN serial bus that connects to the gondola avionics system to allow for ground station monitoring of the battery system.

Solar Panels

SunCat Solar, an Arizona-based company that makes solar panel systems for race cars, has built panels for our ballooning missions since the early 2000s. The panels for both GUSTO and Sunrise III use high-efficiency single-crystal silicon cells.

The panels are provided in two modules of cells arranged as a 4-by-5 array and a 6-by-5 array. For the SBI mission, we used four panels consisting of two 6-by-5 modules and one 4-by-5 module. The cells in the modules are connected in series, and the three modules are then connected in series for a total of 80 cells, producing an open circuit voltage of ~ 55 V.

GUSTO will use eighteen 80-cell panels, while Sunrise III will use six 90-cell panels. Every five cells in both module types have a bypass diode connected across those cells to ensure that, if a cell in the series chain

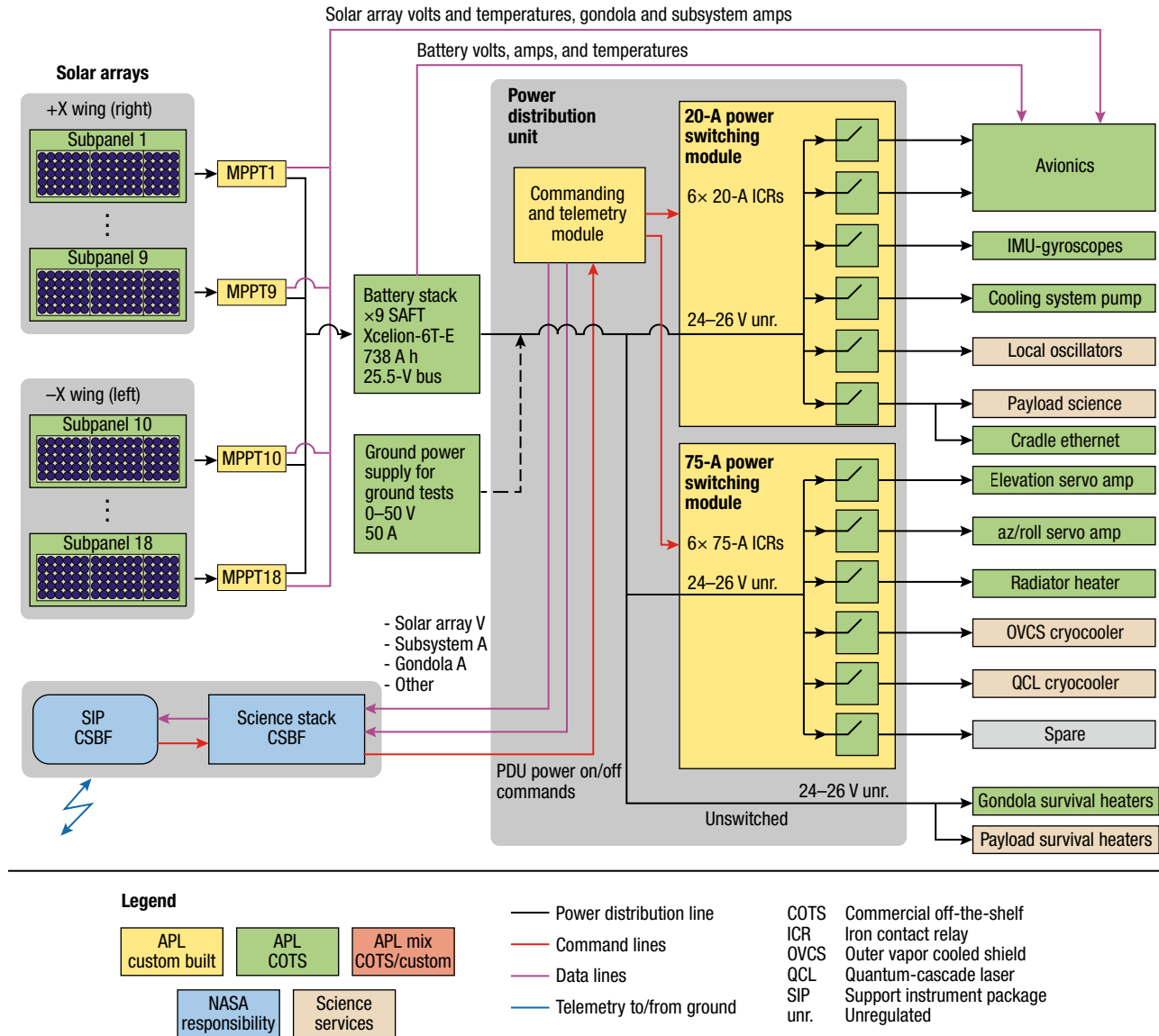


Figure 11. APL-developed power system for the GUSTO balloon mission. The solar arrays power a battery stack made up of lithium cell batteries. The MPPT adjusts the loading of the solar panels and then delivers the power to the battery bus. The PDU distributes the battery power to the various subsystems to ensure they are powered for the duration of the mission.

breaks, the current pathway is maintained by passing the current around the group that contains the broken cell. This allows the panel to continue producing power with only about a 3-V drop in output voltage.

The modules are fabricated on an aluminum honeycomb support. The front of the modules is laminated with a protective film, and the back is covered in a thin sheet of a fiberglass-epoxy material. The entire module is framed around the outer edge in half-inch spruce. This structure provides a lightweight yet rigid structure for the modules. The modules are then placed into an aluminum frame, which is assembled into the final array.

GUSTO has nine panels in each of two large arrays, one mounted on each side of the gondola, for a total of 18 panels (Figure 12).

The total power output would be ~5,000 W if all panels were illuminated at the same time with the Sun shining directly on them. Because of the 22.5° tilt of Earth’s axis, the panels need to be mounted at this angle to maximize their output power. Since GUSTO will avoid pointing directly at the Sun, the large arrays are horizontally angled back from the front of the gondola to keep the Sun shining directly on them.

Sunrise III has six panels, three in each of two large arrays. Since Sunrise will look directly at the Sun, the panels are only tilted at 22.5° off vertical and are not tilted off the front of the gondola.

Since a solar cell is essentially a current source, each panel’s output could be connected directly to the 24-V battery bus, but this would not get the most power from



Figure 12. One of two GUSTO arrays. These high-efficiency panels are key to recharging the high-capacity batteries on GUSTO's planned 75-day mission.

the panels for recharging the batteries. We overcome this limitation by using an MPPT.

Maximum Power Point Tracker

The maximum power point of the solar panel unfortunately is not matched to the typical 24-V battery system (Figure 13).

The MPPT determines where the maximum power point is and adjusts the loading of the solar panel until the product of the panel output voltage and output current are maximized. The MPPT then delivers this power to the battery bus. Since the maximum power point for the solar panel in our case will be at a voltage higher than the battery bus, the MPPT uses a DC-to-DC buck converter to deliver the correct voltage level to the batteries at an output current higher than the input current, thus

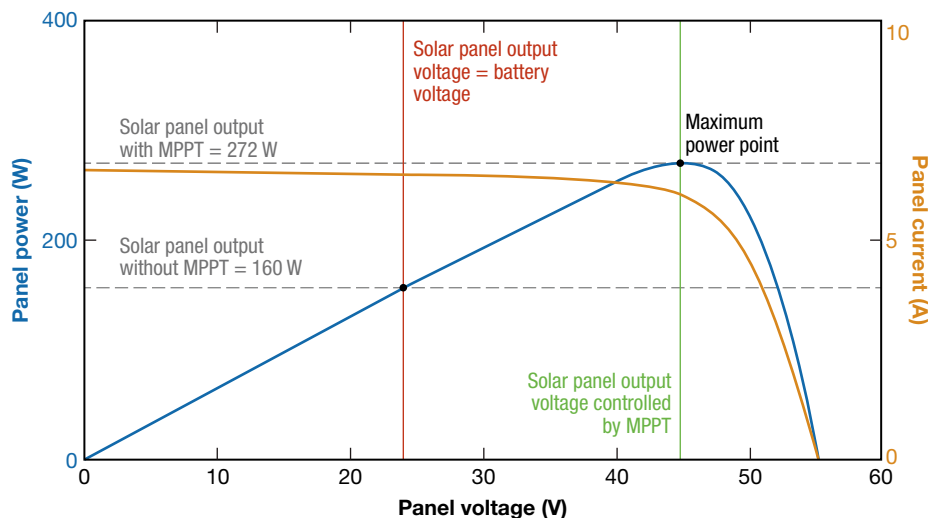


Figure 13. Solar panel power curve. Without using the MPPT, the solar panel output was 160 W; with the MPPT, it was 272 W.

delivering the most power to the batteries. On STO-2, we used a commercial MPPT unit, the TriStar60 manufactured by the Morningstar Corp. The unit is rated for panels producing up to 150 V and currents as high as 60 A. This unit will also fly on Sunrise III. On STO-2, in addition to the TriStar unit, we flew three independent MPPTs designed and built at APL. Each APL unit was attached to a non-mission-critical secondary solar panel, resulting in a qualifying flight for the design (Figure 14).

Independent MPPTs have two distinct advantages. First, a failure of a single MPPT or a complete failure of a single solar panel will not endanger the mission. Second, the APL MPPT is built using a buck/boost DC-to-DC converter technology. This means that as long as a solar panel is producing an output of at least 10 V at any current level, the MPPT will boost the panel voltage up to the battery bus voltage and provide some amount of charging current to the batteries.

In addition to providing the most efficient way to charge the batteries, APL's MPPT also provides information about the output voltage and current of the solar panels and the output voltage and current of the MPPT to the batteries. Four of the MPPTs (which will fly on GUSTO; see Figure 11) are configured to provide this information, as well as panel temperatures and MPPT temperatures. Because the avionics system has a limited number of analog data acquisition channels, the input voltage and current and the output voltage and current are multiplexed to four channels on the avionics system. However, the solar panel temperatures and MPPT temperatures are routed directly to the avionics subsystem.

Power Distribution Unit

The final element in the balloon power system is the PDU (Figure 15), which controls the routing of the battery power to the various subsystems on the gondola. The principal subsystems are

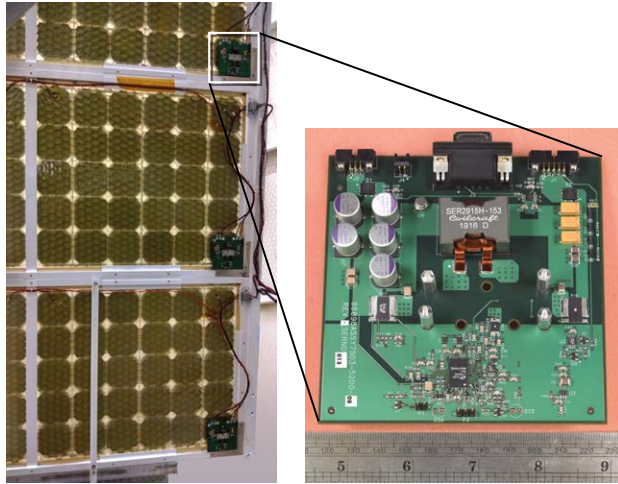


Figure 14. APL-built MPPTs mounted to the three secondary panels on STO-2. This was the design’s qualifying flight. Independent MPPTs guard against mission failure if a single MPPT or a solar panel fails.

avionics, attitude control servos and motors, the science payload, and survival heaters (Figure 11). The PDU also monitors the bus voltage and output currents to the subsystems and delivers this information to the avionics and science stack, a CSBF-provided subsystem for controlling the PDU in flight and monitoring the power system.

APL designed and built the current PDU for the BRRISON mission, and the PDU (Figure 15, left) has since flown on two additional missions, BOPPS and STO-2. It will also fly on the Sunrise III mission.

APL built an enhanced version of the PDU for the GUSTO mission. The original APL PDU has six 20-A relays and six 75-A relays controlled by eight command

signals or the toggle switches on the front panel (see Figure 6). The GUSTO PDU (Figure 15, right) has the same set of relays, but the command signals have been increased to 12 and the front panel switches were removed because of space constraints. The command signals are routed through a steering matrix. This matrix enables multiple relays to be controlled by a single command signal, as is the case with the azimuth, elevation, and roll compensation servos and motors. Any relay operation can be made conditional on other relays being enabled. Specifically, the servo relays cannot be switched on unless the avionics relay is first turned on. This prevents the azimuth, elevation, and roll systems from powering on without the avionics subsystem being able to provide control signals to them.

To provide redundant power system monitoring, information regarding battery bus voltage, battery charging or discharging current, total current being supplied to the gondola, total current through all 20-A and 75-A relays, and total current through an unswitched auxiliary bus is sent to the avionics subsystem and the science stack. Light-emitting diodes on the front panel indicate which subsystems are on or off. A digital front panel also displays this information. Before the solar arrays are attached, the PDU allows for recharging the batteries from a ground support equipment (GSE) power supply. The charging current is routed through the set of GSE charging diodes.

FIELD AND MISSION OPERATIONS

A common location for scientific balloon launches is McMurdo Station in Antarctica (Figure 16). Launching from such a remote location presents many logistical

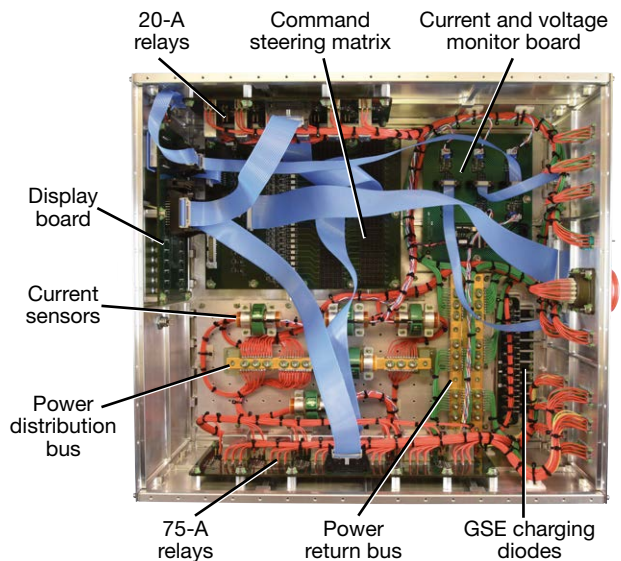


Figure 15. PDU used in several missions. Left, PDU flown on BOPPS, STO-2, and Sunrise III. Right, interior of the newly built GUSTO PDU. The PDU controls the routing of battery power to the subsystems. The GUSTO PDU has the same set of relays but an increased number of command signals.



Figure 16. Balloon facilities. Left, NASA balloon facility near the Ross Ice Shelf near McMurdo, Antarctica; right, McMurdo Station; bottom, STO-2 peeking out of one of the integration hangars.

and operational challenges; however, it also has distinct advantages.

Launching at an extreme southern latitude during the Antarctic summer means that the Sun never sets during the mission. The 24-h daylight provides ample energy for power-hungry science instruments; it also allows the gondola to avoid extreme temperature drops that would occur at night. Such temperature drops could require heaters for system components to prevent damage from freezing. Adding heaters could also lead to a cascade of additional design challenges. Heaters draw a significant amount of power when running; without sunlight, that requires more energy storage (i.e., batteries). Batteries are heavy, so the more batteries needed, the more challenging it is to meet the gondola design's weight limitations. Therefore, constant daylight throughout a mission is beneficial.

Another distinct advantage of launching from Antarctica is the predictable flight path. In December, the winds in the stratosphere reliably form an anticyclone around the South Pole, and it lasts anywhere from a few weeks to a month. The anticyclone usually results in the balloon completing a circular trajectory around the South Pole in about 14 days (Figure 17). The balloon remains over land, which allows for the payload to be recovered after the mission ends. Recovering scientific payloads is usually a mission requirement, not only so that expensive scientific equipment can be refurbished and reused but also so that the data gathered during the mission can be retrieved. The amount of data gathered typically far exceeds the system's telemetry bandwidth capabilities, so the data gathered are often stored on hard drives and other nonvolatile storage media that need to be physically recovered.

Launching scientific balloons from Antarctica also presents plenty of challenges. Because Antarctica is one

of the most remote places on Earth (and has one of the harshest climates), getting equipment and people there is difficult. All equipment and people follow the same route to McMurdo. First, everything must make its way to Christchurch, New Zealand. From there, the US military provides flights to and from McMurdo. The largest aircraft that can make the journey between New Zealand and McMurdo is a C-17 jet, meaning all project equipment must be disassembled and packed to fit on a C-17.

It is also important to pack everything the project needs (or might need!). Antarctica does not have the convenience of next-day delivery that many have come to rely on to keep projects on schedule. If a component is missing or broken, it could take weeks for a replacement to make it to Antarctica, even if a replacement is readily available in the continental United States. Flights to and from Antarctica are so dependent on weather that even if a flight has departed New Zealand, weather could force it to turn around (known as “boomeranging”). Landing conditions in Antarctica can change dramatically and quickly, and predicting the weather conditions there is

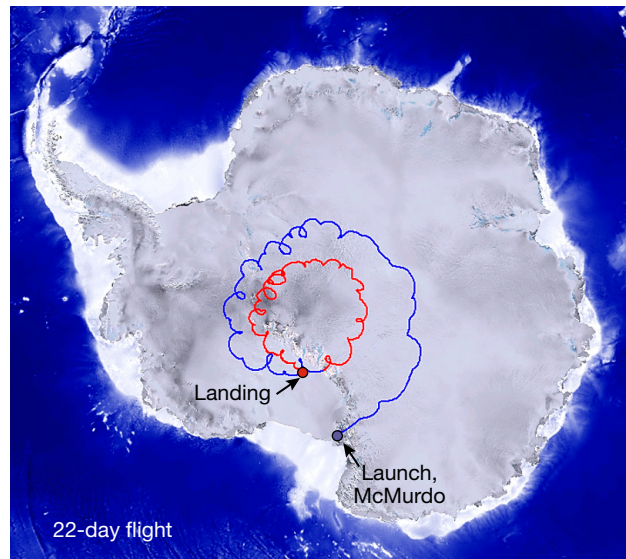


Figure 17. STO-2 flight path over Antarctica. The flight season in Antarctica is relatively short and depends on the presence of an anticyclone in the stratosphere. Over the course of the mission, the balloon stays over land, and the team recovers it at the landing site.

notoriously difficult. The flight from New Zealand to McMurdo takes about 8 h, which is more than enough time for the weather to deteriorate. Weather unsuitable for landing aircraft could last hours, days, or weeks. A delay can be devastating for the mission, especially since the anticyclone is only available for a relatively short time. When the anticyclone weakens and dissipates, the launch window for the season closes, and any balloon projects not yet launched will have to wait until next year.

Another challenge for Antarctic field missions is limited data connectivity. Antarctica is the only continent on Earth that does not have a high-speed fiber optic cable network connecting it to the outside world. Currently, McMurdo relies on low-bandwidth satellite systems to provide internet connectivity to personnel stationed there. The total bandwidth is less than what two 4G cell phones are capable of, and it is shared among up to 1,000 people on base during the Antarctic summer. This creates significant bottlenecks for sending and receiving data, highlighting the importance of having skilled and knowledgeable personnel on-site. While it is still possible to send emails and have phone conversations, other forms of remote support are typically not possible.

The facilities at McMurdo where gondolas are assembled, integrated, and tested are unique. They are off the main base and located on the Ross Ice Shelf. Because of this, the integration building is literally on skis (Figure 16), and it is moved each year to prevent it from sinking into the ice shelf. The building is relatively small (compared with typical integration facilities) and only has a single-axis crane. Its floors are wooden and heated. In contrast to concrete floors, the wood floor has pressure limitations, making it important to consider the gondola's weight distribution. The gondola is designed so that it can be assembled and tested within the footprint and limitations of this building.

When the gondola is fully assembled and compatibility testing has been completed, the payload is ready to launch. Two conditions must be satisfied for a launch attempt: the anticyclone in the stratosphere must have formed, and ground conditions need to be ideal. For a scientific balloon launch, there are strict limitations on wind conditions. Winds must be calm, and wind shear forces in the air column must be insignificant. Wind shear can easily tear the balloon

during ascent and immediately end the mission. Suitable launch conditions can be hard to come by, so the team is on call for 24 h in case weather predictions suggest a possible launch opportunity.

If weather conditions are satisfactory, the launch attempt is approved and the gondola is transported to the launchpad. The balloon is prepped and attached to the gondola. The balloon is filled with helium and released. If all goes well, the balloon and its gondola begin ascending through the atmosphere. In about 3 h, the gondola will reach its float altitude of ~120,000 ft and science observations can begin.

Once the scientific balloon has launched, operators must monitor and command the system through the duration of the flight. This typically involves a cadre of project personnel both at McMurdo and APL. Even with the internet limitations present at McMurdo, the team is usually small enough that those who traveled there need to stay until the flight's end to support and monitor the system. It takes a team effort for 24/7 operations.

Most system operations on the gondola are automated out of necessity. For much of the flight, telemetry data from the gondola travel through a network of satellite systems that can add significant latency. This means that what an operator sees at their ground station has often occurred several minutes before, and any command the operator sends could take several minutes to be received. It is up to the gondola software to prevent and avoid mission-ending scenarios (e.g., for astrophysics missions, pointing the telescope at the Sun would cause mission-ending damage to the system).

However, not every scenario can be predicted, managed, and avoided by software, so constant human oversight is still needed. Unexpected events do occur during balloon missions. During the STO-2 flight, a slow coolant leak required an operator to take over thermal



Figure 18. Landings of three APL balloon gondolas in Antarctica. The goal is a soft (i.e., snowy) landing so that the gondola remains mostly in one piece and data storage and other components can be easily recovered.

management. The operator had to adjust the gondola's azimuth periodically to vary and limit what system components were in the Sun's direct path to avoid system damage from overheating.

Another unexpected event during the STO-2 flight was a suspected cosmic ray bit flip, which crippled the functionality of a flight computer. Components on a balloon mission are not often space-rated because of cost and availability restrictions. One advantage of ballooning is that there is still some protection from the harsh space environment, making such events unlikely. However, these radiation events can still occur. On STO-2, an operator had to induce power cycling to restore the computer's functionality.

A scientific balloon flight ends with a termination command sent from the ground. The decision to initiate a terminate sequence involves many factors, but the most important is where the gondola will land. Termination is timed to make payload recovery operations as easy and safe as possible. When the balloon passes over an ideal landing location, the current status of the mission is weighed against the probability of another suitable termination condition (often dependent on the state of the anticyclone). Whether or not the science goals have been achieved, the supply of mission consumables (e.g., a cryogen), and the probability of continued success or failure are taken into account.

After the decision to end the flight, the terminate command sets off a reaction that tears the balloon, releasing the helium and sending the gondola into a free-fall back to Earth. A parachute in line with the flight train self-inflates as the air density increases during decent, slowing the gondola's speed before impact. With a bit of luck, the gondola will have a soft (i.e., snowy) landing spot, and it will remain mostly in one piece (Figure 18). Then recovery operations begin. A team is deployed to recover the data storage systems on the gondola and the rest of its components. Ultimately, the team aims to return as much of the gondola and its systems as possible to McMurdo. Once back at McMurdo, the gondola can be disassembled and transported back to the United States and APL. The mission observation data are provided to the project scientists for analysis, and the gondola components are refurbished so they can be used on the next mission.

CONCLUSION

Our team at APL, in collaboration with the Lab's Space Exploration Sector, has enabled unprecedented pointing accuracy and stability, facilitating otherwise impossible missions. We have also been responsible for much of the developmental work required for all of APL's long-duration balloon projects. These efforts include avionics, power systems, software, command and control, ground support, systems engineering, integration,

and testing. In addition, REDD has provided fabrication and design work for electrical and mechanical systems development. Still a modest portion of the Space Exploration Sector's portfolio, stratospheric ballooning has been a steadily growing business at APL due in large part to major contributions from REDD.

ACKNOWLEDGMENTS: The authors acknowledge the many contributions from those in APL's Space Exploration Sector program management who have worked tirelessly to win missions and oversee execution of programs in this area. In addition, many other staff members from both REDD and the Space Exploration Sector have made significant contributions to the success of stratospheric ballooning programs; these include mechanical design and fabrication, electronics fabrication, materials development, and mission assurance experts among others.

REFERENCES

- ¹D. M. Rust, J. R. Hayes, D. A. Lohr, G. A. Murphy, and K. Strohhahn, "The Flare Genesis Experiment: Studying the Sun from the stratosphere," *Johns Hopkins APL Tech. Dig.*, vol. 14, no. 4, pp. 358–369, 1993, <https://secwww.jhuapl.edu/techdigest/Content/techdigest/pdf/V14-N04/14-04-Rust.pdf>.
- ²P. N. Bernasconi, D. M. Rust, B. J. LaBonte, and M. K. Georgoulis, "Science-driven innovation: Developing the right tools for solar research," *Johns Hopkins APL Tech. Dig.*, vol. 26, no. 2, pp. 132–142, 2005, <https://secwww.jhuapl.edu/techdigest/Content/techdigest/pdf/V26-N02/26-02-Bernasconi.pdf>.
- ³J. Adkins (Ed.), "Types of balloons," NASA, last updated May 17, 2022, <https://www.nasa.gov/scientific-balloons/types-of-balloons>.
- ⁴T. Kremic, A. F. Cheng, K. Hibbits, E. F. Young, R. R. Ansari, et al., "Stratospheric balloons for planetary science and the Balloon Observation Platform for Planetary Science (BOPPS) mission summary," In *Proc. 2015 IEEE Aerosp. Conf., Big Sky, MT, 2015*, pp. 1–10, <https://doi.org/10.1109/AERO.2015.7119008>.
- ⁵P. N. Bernasconi, D. M. Rust, and H. A. C. Eaton, "High resolution vector magnetograms with the Flare Genesis vector polarimeter," in *Advanced Solar Polarimetry—Theory, Observation, and Instrumentation: 20th NSO/SAC Summer Workshop*, vol. 236, pp. 399–406, 2001, <https://www.aspbbooks.org/publications/236/399.pdf>.
- ⁶P. Foukal, P. Bernasconi, H. Eaton, and D. Rust, "Broadband measurements of facular photometric contrast using the Solar Bolometric Imager," *Astrophys. J.*, vol. 611, no. 1, art. L57, 2004, <https://doi.org/10.1086/423787>.
- ⁷P. N. Bernasconi, D. Neufeld, C. Walker, D. Hollenbach, J. Kawamura, and J. Stuzki, "The Stratospheric Terahertz Observatory," *Johns Hopkins APL Tech. Dig.*, vol. 28, no. 3, pp. 238–239, 2010, <https://secwww.jhuapl.edu/techdigest/Content/techdigest/pdf/V28-N03/28-03-Bernasconi.pdf>.
- ⁸Y. M. Seo, P. F. Goldsmith, C. K. Walker, D. J. Hollenbach, M. G. Wolfire, et al., "Probing ISM structure in Trumpler 14 and Carina I using the Stratospheric Terahertz Observatory 2," *Astrophys. J.*, vol. 878, no. 2, art. 120, 2019, <https://doi.org/10.3847/1538-4357/ab2043>.
- ⁹E. Kassarian, F. Sanfedino, D. Alazard, H. Evain, and J. Montel, "Modeling and stability of balloon-borne gondolas with coupled pendulum-torsion dynamics," *Aerosp. Sci. Technol.*, vol. 112, art. 106607, 2021, <https://doi.org/10.1016/j.ast.2021.106607>.
- ¹⁰K. D. DeWeese and P. R. Ward, "Demonstration of a Balloon borne arc-second pointer design," in *Proc. 36th COSPAR Scientific Assem.*, <https://ntrs.nasa.gov/citations/20080039319>.
- ¹¹D. Huguenin, "Design and performance of stratospheric balloon-borne platforms for infrared astrophysical observations," *Infrared Phys. Technol.*, vol. 35, nos. 2–3, pp. 195–202, 1994, [https://doi.org/10.1016/1350-4495\(94\)90080-9](https://doi.org/10.1016/1350-4495(94)90080-9).

- ¹²B. M. Quine, V. Tarasyuk, H. Mebrahtu, and R. Hornsey, "Determining star-image location: A new sub-pixel interpolation technique to process image centroids," *Comput. Phys. Commun.*, vol. 177, no. 9, pp. 700–706, 2007, <https://doi.org/10.1016/j.cpc.2007.06.007>.
- ¹³A. S. Szalay, J. Gray, G. Fekete, P. Z. Kunszt, P. Z. Kukol, and A. Thakar, "Indexing the sphere with the hierarchical triangular mesh," Tech. Rep. MSR-TR-2005-123, Microsoft, Sep. 2005, <https://www.microsoft.com/en-us/research/publication/indexing-the-sphere-with-the-hierarchical-triangular-mesh/>.
- ¹⁴A. Likas, N. Vlassis, and J. J. Verbeek, "The global k -means clustering algorithm," *Pattern Recognit.*, vol. 36, no. 2, pp. 451–461, 2003, [https://doi.org/10.1016/S0031-3203\(02\)00060-2](https://doi.org/10.1016/S0031-3203(02)00060-2).
- ¹⁵M. D. Shuster, "The optimization of TRIAD," *J. Astronaut. Sci.*, vol. 55, pp. 245–257, 2007, <https://doi.org/10.1007/BF03256523>.



E. Brian Alvarez, Research and Exploratory Development Department, Johns Hopkins University Applied Physics Laboratory, Laurel, MD

E. Brian Alvarez is the group supervisor of the Electrical Engineering Systems Analysis and Design Group at APL. He has a BS in electrical engineering from the University of Maryland and an MS in technical management from Johns Hopkins University. Before becoming a supervisor, he was an electrical and systems engineer and worked on several flight instrumentation and data collection/analysis systems for spacecraft. As group supervisor, he is responsible for strategy, staffing, structure, and operations for teams that provide electrical engineering for agile systems and sensing, embedded systems, and electrical design for fabrication. His email address is brian.alvarez@jhuapl.edu.



Harry A. Eaton, Research and Exploratory Development Department, Johns Hopkins University Applied Physics Laboratory, Laurel, MD

Harry A. Eaton is a gondola systems engineer and section supervisor in the Electrical Engineering Systems Analysis and Design Group at APL. He has a BS in electrical engineering from Colorado State University and an MS in electrical engineering from Johns Hopkins University. He developed an improved pointing control system for the Balloon Rapid Response for ISON (BRRISON) mission that included actuator controls, inertial measurement, attitude estimation, and a unique pendulum damping system. He also developed software for gondola controls and oversaw all gondola subsystems. He has extensive electronics engineering experience, including analog circuit design, digital circuit design, and software development, as well as all phases of circuit and system design from conception to production, testing, and field use. His email address is harry.eaton@jhuapl.edu.



Michael S. Carpenter, Research and Exploratory Development Department, Johns Hopkins University Applied Physics Laboratory, Laurel, MD

Michael S. Carpenter is an electrical and systems engineer in the Electrical Engineering Systems Analysis and Design Group at APL. He has a BS in computer engineering from Michigan State University and an MS in electrical and computer engineering from Johns Hopkins University. He developed pointing control software for the Stratospheric Terahertz Observatory (STO)-2 mission and was part of the integration team in McMurdo during both the 2015 and

2016 campaign seasons. He is the lead gondola engineer for the Sunrise III mission. His email address is michael.carpenter@jhuapl.edu.



Bliss G. Carkhuff, Research and Exploratory Development Department, Johns Hopkins University Applied Physics Laboratory, Laurel, MD

Bliss G. Carkhuff is an electrical engineer in the Electrical Engineering Systems Analysis and Design Group at APL. He has a BE in electrical engineering and an MS in electrical and computer engineering, both from Johns Hopkins University. He has extensive experience that includes fabrication support and electronics system design and testing, as well as expertise in battery health monitoring for lithium ion battery systems. For the Solar Bolometric Imager (SBI)-II project, he supported a failure investigation and requalification flight. He also worked on the Stratospheric Terahertz Observatory (STO) mission. In 2006, he was honored with APL's Master Inventor award, which recognizes APL staff members with a demonstrated career of innovation by having 10 or more patents based on APL intellectual property. His email address is bliss.carkhuff@jhuapl.edu.



Pietro N. Bernasconi, Space Exploration Sector, Johns Hopkins University Applied Physics Laboratory, Laurel, MD

Pietro N. Bernasconi is a research scientist, balloon systems engineer, and balloon project manager in the Space Physics Group at APL. He has an MS in physics and a PhD in natural science, both from the Swiss Federal Institute of Technology in Zurich, Switzerland. He has an extensive background in physics, optics, and computer programming, which he has applied to a variety of scientific balloon missions. He was a project scientist on the Flare Genesis Experiment (FGE) mission, for which he developed and tested the postfocus optics and command and control software, as well as other electrical and mechanical components. He was also a project scientist and the principal investigator on the Solar Bolometric Imager (SBI) mission. He led the APL team for the Stratospheric Terahertz Observatory (STO) mission and was mission systems engineer for the Galactic/Extragalactic ULDB Spectroscopic Terahertz Observatory (GUSTO). For Balloon Rapid Response for ISON (BRRISON)/Balloon Observation Platform for Planetary Science (BOPPS), he serves as the gondola lead engineer and also developed command and control software and assisted the project manager and mission systems engineer. He leads the APL team for STO-2 and is developing the command and control software. His email address is pietro.bernasconi@jhuapl.edu.